J Mater Sci (2011) 46:1132–1135
DOI 10.1007/s10853-010-4991-5

LETTER

Increasing the thermal diffusivity of flexible graphite sheets by superheated steam treatment

Satoshi Kitaoka · Masashi Wada · Takahiro Nagai · Noburou Osa · Takayoshi Konno

Received: 14 June 2010 / Accepted: 6 October 2010 / Published online: 20 October 2010
© Springer Science+Business Media, LLC 2010

Flexible expanded graphite sheets are used as thermal interface materials for heat dissipation in electronic devices such as CPU packages [1] and LEDs [2], because the graphite sheets have a high thermal conductivity, are lightweight, and can conform well to surfaces. Sheets made of natural graphite are generally fabricated by the following process. Natural flake graphite is initially soaked in intercalating agents such as concentrated sulfuric acid and perchloric acid along with potassium dichromate or nitric acid oxidizing agents to intercalate the reagent ions into the interlayer spaces of the graphite. The graphite is then washed with water to remove excess reagent, and dried. Then, the intercalated graphite is expanded significantly by heat treatment above 1000 K, during which the graphene layers are exfoliated by thermal vaporization of the intercalants. Graphite sheets are mechanically formed by roll-compacting the expanded graphite flakes without binders [3, 4].

It is well known that a wide variety of functional groups containing oxygen and hydrogen are formed at structural imperfections on the graphite surfaces after soaking in oxidizing solutions such as sulfuric acid, nitric acid, or $(NH_4)_2S_2O_8$ [5, 6]. Therefore, there should be many functional groups on the expanded graphite surfaces of the above-described flexible sheets. These functional groups should promote phonon scattering at the contact interfaces of the graphite crystals and reduce the thermal conductivity of the sheets. The thermal conduction of the sheets can usually be increased by heat treatment in vacuum up to about 1300 K over a long time, since such treatment dissipates the chemically adsorbed layers. However, such batch treatment has low production efficiency. It is thus highly desirable to develop a low-cost technique suitable for continuous mass production.

There has been vigorous investigation of the high-temperature oxidation of graphite. For example, the carbon-steam reaction is an important reaction for many industrial processes, including coal gasification and activation of carbon [7–9]. This reaction is considered to have the following mechanism.

$$\begin{aligned} &C + H_2O \rightarrow C(O) + H_2 \\ &C + \frac{1}{2}H_2 \leftrightarrow C(H) \\ &C(O) \rightarrow CO \end{aligned} \tag{1}$$

where the parentheses indicate elements chemically adsorbed on the carbon surface. Dissociative chemisorption of H_2 mainly proceeds at 973 K, and is believed to occur preferentially on zigzag faces over armchair faces of graphite and to proceed more complete at low temperatures. If exposure to steam below 973 K effectively removes some of the large oxygen-containing functional groups (such as carbonate, carboxyl, and lactone) and forms the graphite surfaces chemisorbed with hydrogen,

S. Kitaoka (✉) · M. Wada
Japan Fine Ceramics Center, 2-41 Mutsuno, Atsuta-ku, Nagoya 456-8587, Japan
e-mail: kitaoka@jfcc.or.jp

T. Nagai
Daido Corporation, 3-8 Shimosawa-machi, Tajimi 507-0812, Japan

N. Osa
Energy Application Research and Development Center, Chubu Electric Power Company, 20-1 Kitasekiyama, Ohdaka-cho, Midori-ku, Nagoya 459-8522, Japan

T. Konno
KFK Corporation, 1-17-43 Yada-cho, Higashi-ku, Nagoya 461-0040, Japan

phonon scattering at the graphite contact interfaces will be suppressed, thereby increasing the thermal conductivity of the sheets. In contrast, at temperatures above 973 K, graphite is rapidly dissipated through the evolution of CO, resulting in the formation of porous sheets in a process similar to that used to produce activated carbons using steam. It reduces the thermal conductivity of the sheets.

This study examined the relationship between the temperature of the superheated steam in the above process and the thermal diffusivity of the resulting flexible expanded graphite sheets. Flexible graphite sheets were produced by roll-compacting exfoliated graphite particles, which were expanded by soaking natural flake graphite in oxidizing agents. The oxidizing agents were intercalated into the interlayer spaces of the graphite, and subsequently thermally vaporized. The sheets were about 300-μm thick, and their apparent density was 1100–1200 kg/m^3. X-ray diffraction profiles of the sheets indicated that they were highly oriented, with their (001) lattice planes parallel to the sheet surface. The lattice constant c_0 (002) and the crystallite size L_c (002) along the c-axis were 0.671 nm and approximately 40 nm, respectively. c_0 (002) and the corresponding half-width of the diffraction peak for the sheets were the same as those of the exfoliated graphite particles, indicating that the roll-compaction introduced very little residual strain. Because the sheets were made of natural graphite, they contained various minerals, major components of silicate and sulfur. The amounts of impurity elements in the sheets were measured by inductively coupled plasma spectrometry for Si, Na, K, Ca, Fe, Mn, and Al, and by fluorescent X-ray analysis for S and Zn. The total amount of these elements was about 0.25 wt%. The sheets were cut into 200 × 200 mm specimens. Each specimen was installed in a holding jig, and the plane of the sheet was orientated at a 45° angle to the steam flow. The specimen was then exposed to superheated steam at a flow rate of 10 kg/h. The superheated steam was produced by induction heating of saturated steam prepared at about 400 K for 10 min at 723, 773, and 823 K. The heating and cooling rates were 10 and 30 K/min, respectively.

The in-plane thermal diffusivity of each specimen (which was highly orthotropic in two dimensions) was measured by an AC calorimetric technique that employed laser heating [10]. In the AC technique, a uniform laser beam was irradiated upon the specimen surface, and the phase lag and amplitude of the thermal wave were measured using a thermocouple on the rear surface. Two types of thermal diffusivity were determined from the slopes of the relation of the phase lag and the relative distance between the heating point and the detection point and the relation of the amplitude and the relative distance. In this study, the geometric mean value of the thermal diffusivities was used as the in-plane thermal diffusivity of the graphite sheets.

Figure 1 shows the thermal diffusivity of the graphite sheets as a function of the superheated steam temperature. The solid circle indicates the diffusivity of an untreated sheet. Ten specimens were measured for each steam temperature. The thermal diffusivity obviously increased with increasing steam temperature up to 773 K, after which it reached a plateau. The standard deviation of the data for the treated specimens was two to three times that of the untreated specimens (0.1). Since the relative density of the

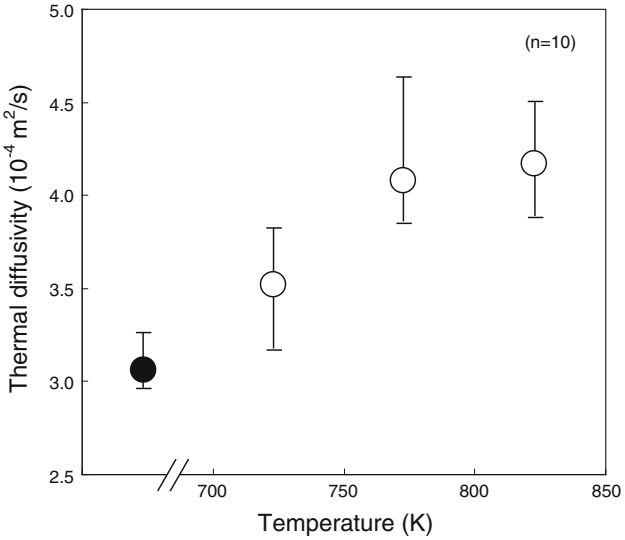

Fig. 1 Thermal diffusivity of graphite sheets as a function of superheated steam temperature (treatment time: 10 min). The *solid circle* indicates the diffusivity before the superheated steam treatment

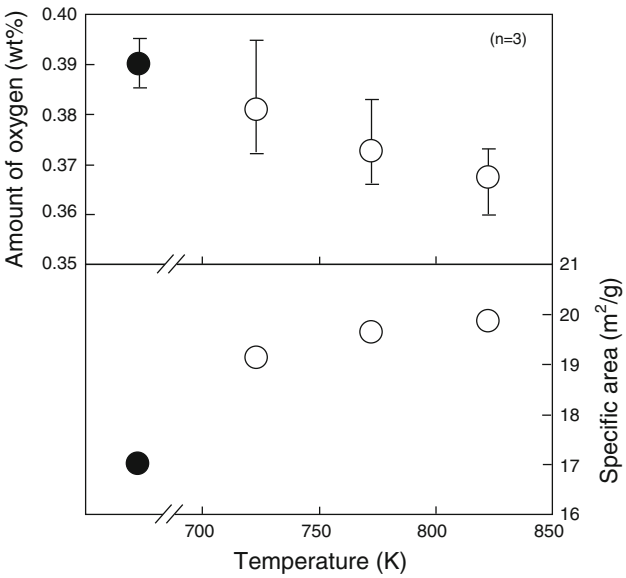

Fig. 2 Amount of oxygen and specific area of graphite sheets as a function of superheated steam temperature (treatment time: 10 min). The *solid circles* indicate the values before the superheated steam treatment

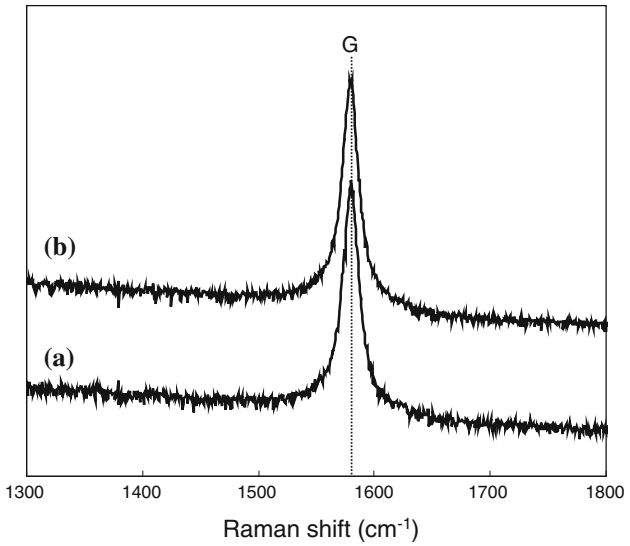

Fig. 3 Raman spectra of the graphite sheet surfaces **a** before and **b** after superheated steam treatment at 773 K for 10 min

sheets was almost the same during steam treatment, the thermal conductivity of the sheets must therefore have been increased by the treatment.

The total amount of oxygen in each specimen was measured by inert-gas fusion/infrared absorption spectroscopy, and the specific surface area of each specimen was determined by the BET method using N_2 adsorption. Figure 2 shows the total amount of oxygen (the average of three measurements for each specimen) and the specific area of the specimens as a function of the superheated steam temperature. The total amount of oxygen clearly decreased with increasing temperature, but even at 823 K it was only about 5% less than that of the untreated specimen. The individual amounts of impurity elements such as Si, Na, K, Ca, Fe, Mn, Al, S, and Zn after the steam treatment were similar to those before the treatment. Even if all of the quantified elements existed as oxides, the corresponding total amount of oxygen was only approximately 0.1 wt%. Therefore, the detected oxygen, shown in Fig. 2, was primarily adsorbed on the graphite surfaces to produce the oxygen-containing functional groups, and some of these remained despite the steam treatment at 823 K. As shown in Fig. 2, the specific surface area after treatment was clearly greater than that before treatment, and gradually increased with increasing temperature. The variation of the specific surface area had little influence on the apparent density of the sheets. The crystallographic parameters c_0 (002) and L_c (002), which were determined from XRD analysis of the sheets, depended little on the steam temperature. The microcrystalline planar size L_a (110) may have been decreased by the steam treatment.

Figure 3 shows Raman spectra of the graphite sheet surfaces before and after superheated steam treatment at 773 K for 10 min. In the Raman spectra obtained using a 514-nm Ar-ion laser, only the G band at 1580 cm^{-1}, which is associated with the stretching vibration mode (E_{2g}) of the infinite graphite basal planes, was observed for all of the sheets. However, the D band at 1360 cm^{-1}, which was assigned to the vibration mode (A_{1g}) originating from disordered structures in the basal layer, such as edges and lattice vacancies, was not detected. The shift and full-width at half maximum of the G band, which were indicative of

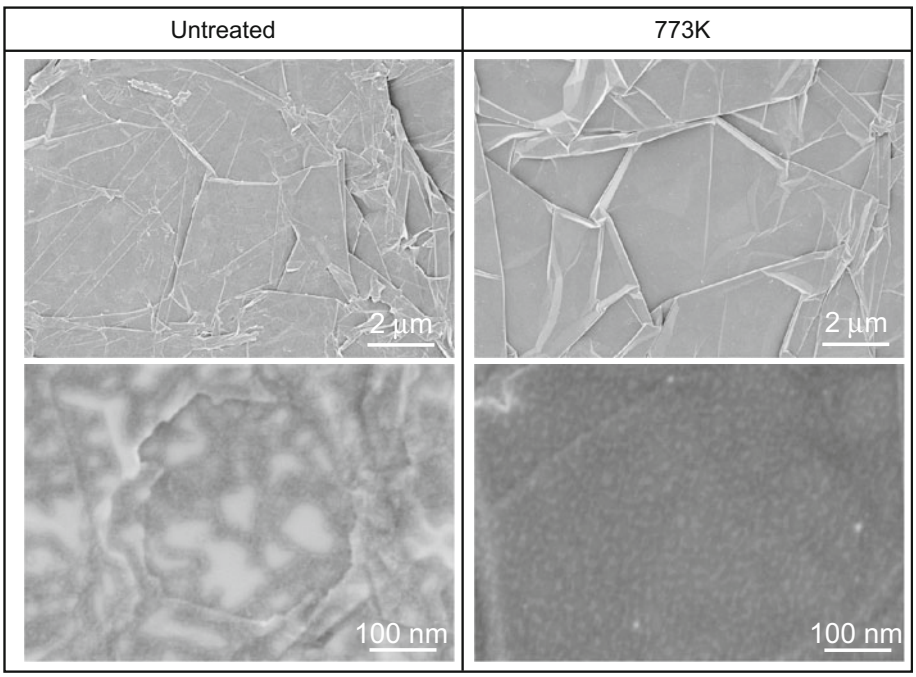

Fig. 4 Scanning electron micrographs of the graphite sheet surfaces **a** before and **b** after superheated steam treatment at 773 K for 10 min

defects in the lattice [11], were not significantly changed by the steam treatment. Furthermore, C 1*s* and O 1*s* X-ray photoelectron spectra obtained using a spectrometer with a monochromatized Al-Kα X-ray anode (1486.6 eV) and FT-IR spectra (reflection mode) were almost the same for all of the sheets, regardless of the steam treatment they received.

Figure 4 shows scanning electron micrographs of graphite sheet surfaces before and after superheated steam treatment at 773 K for 10 min. These backscattered electron images were obtained using an ultralow operating voltage of 0.8 kV to minimize damage to the specimen surfaces by the electron beam. The low-magnification images of steam-treated specimens clearly revealed creases on the sheet surfaces. It was noteworthy that there were many light regions over the entire surface of the untreated sheet, but that these regions shrank after treatment at 773 K, even though no difference was observed in the surface spectral analyses of the sheets before and after the steam treatments. Because the total amount of oxygen in the sheets decreased with increasing treatment temperature, as shown in Fig. 2, the light regions on the untreated sheet were presumed to correspond to regions containing oxygen, which was produced during the sheet preparation and was partly desorbed during steam treatment. However, the actual configuration of this adsorbed oxygen is unclear. The increase in thermal diffusivity due to steam treatment, as shown in Fig. 1, may have been caused by a slight variation of the graphite crystal surfaces, in which the oxygen-containing regions may have been dissipated by irradiation during the XPS and Raman spectral analysis. Such surface modification was probably related to relaxation of phonon scattering at the contact interfaces of the graphite crystals, resulting in improvement of the thermal diffusivity.

References

1. Chung DDL (2006) Adv Microelectron 33(4):8
2. Petrosk J, Norley J, Schober J, Reis B, Reynolds RA (2010) 12th IEEE intersociety conf. on thermal and thermomechanical phenomena in electronic systems, (ISBN: 978-1-4244-5342-9)
3. Wei XH, Liu L, Zhang JX, Shi JL, Guo QG (2010) J Mater Sci 45:2449. doi:10.1007/s10853-010-4216-y
4. Li JH, Feng LL, Jia ZX (2006) Mater Lett 60:746
5. Eli YE, Koch VR (1997) J Electrochem Soc 144:2968
6. Wu YP, Jiang C, Wan C, Holz R (2003) Electrochim Acta 48:867
7. Duan RZ, Yang RT (1984) Chem Eng Sci 39:795
8. Yang RT, Yang KL (1985) Carbon 23:537
9. Chu X, Schmidt LD (1992) Surf Sci 268:325
10. Hatta I (1997) Thermochim Acta 300:7
11. Ko TH, Kuo WS, Chang YH (2000) Polym Compos 21:745